nature microbiology

LETTERS

https://doi.org/10.1038/s41564-019-0567-6

Environmental stimuli drive a transition from cooperation to competition in synthetic phototrophic communities

Cristal Zuñiga[1], Chien-Ting Li[2], Geng Yu[2], Mahmoud M. Al-Bassam[1], TingTing Li[2], Liqun Jiang[2], Livia S. Zaramela[1], Michael Guarnieri[3], Michael J. Betenbaugh[2] and Karsten Zengler[1,4,5*]

Phototrophic communities of photosynthetic algae or cyanobacteria and heterotrophic bacteria or fungi are pervasive throughout the environment[1]. How interactions between members contribute to the resilience and affect the fitness of phototrophic communities is not fully understood[2,3]. Here, we integrated metatranscriptomics, metabolomics and phenotyping with computational modelling to reveal condition-dependent secretion and cross-feeding of metabolites in a synthetic community. We discovered that interactions between members are highly dynamic and are driven by the availability of organic and inorganic nutrients. Environmental factors, such as ammonia concentration, influenced community stability by shifting members from collaborating to competing. Furthermore, overall fitness was dependent on genotype and streamlined genomes improved growth of the entire community. Our mechanistic framework provides insights into the physiology and metabolic response to environmental and genetic perturbation of these ubiquitous microbial associations.

Light-driven microbial communities are highly abundant and inhabit nearly every terrestrial and aquatic environment exposed to light[1]. These communities are either spatially highly structured, such as the ones found in biofilms, microbial mats or lichens[4], or form loose associations, such as aquatic bacteria with phytoplankton[5]. Phototrophic communities consist of photosynthetic organisms that capture light energy and heterotrophic organisms that benefit from photosynthetically fixed carbon. The way in which phototrophic and heterotrophic partners interact and respond to environmental changes has not been fully understood[6]. For example, lichens can interact mutualistically, competitively or parasitically depending on their partners[7,8]. There is a lack of in-depth knowledge about the drivers of these interactions and the metabolic mechanisms underlying cell communication in light-driven communities.

Research of photosynthetic communities is often restricted by the stability of cultures in isolation, their potentially slow growth and the lack of genetic systems for individual partners[9,10]. Evaluating complexity of natural communities with high reproducibility, tractability and accessibility has recently become feasible through the use of model systems for microbial communities[11,12]. Synthetic communities consisting of photoautotrophic and heterotrophic members can mimic basic characteristics of phototrophic communities, thereby providing knowledge about the biology of these symbionts. Two-species experimental systems populated by phototrophs and heterotrophs have provided insight into ecological niches[13] and guided bioproduction approaches[14].

Community metabolic (CM) models have become available for contextualization of multi-omics data[2,15]. Here, a systems biology approach using constraint-based CM models in conjunction with multi-omics and growth physiology experiments was applied to elucidate the phototrophic community comprising the alga *Chlorella vulgaris* (hereafter referred to as alga) and the ascomycete *Saccharomyces cerevisiae* (that is, the fungus). The CM model *i*CZ-CvSc(1748) enables systematic studies related to fitness, maintenance and resilience to environmental and genetic perturbations, using flux balance analysis formulation (equation 1). We experimentally corroborated predictions of growth rates, metabolite exchanges and genome content using physiological data, targeted metabolomics and expression data to systematically reveal governing constraints on cross-feeding, community yields and types of interactions.

Constraint-based models compile metabolic knowledge into a mathematical framework that enables a mechanistic description of physiology based on biological functions (constraints) determined experimentally. Using individual genome-scale metabolic models of *C. vulgaris*, *i*CZ843 (ref. [16]) and *S. cerevisiae*, *i*MM904[17], a phototrophic CM model, *i*CZ-CvSc(1748) was assembled (Supplementary Table 1). The ability of each member to exchange metabolites into the shared metabolite pool (SMP, consisting of 53 alga- and 164 fungus-associated metabolites), was manually curated using experimental data (Supplementary Table 2).

Despite previous studies reporting ineffective co-cultivation of *C. vulgaris* and *S. cerevisiae*[13], we established reproducible cultivation conditions (Supplementary Fig. 1) using the reconstructed *i*CZ-CvSc(1748) model. Model properties and constraints are given in Supplementary Table 3. Experimental growth rates of the alga and fungus ranged between $0.038 \pm 0.006\,h^{-1}$ and $0.034 \pm 0.006\,h^{-1}$, whereas simulated growth rates were $0.041\,h^{-1}$ for the algae and $0.032\,h^{-1}$ for the fungus (Fig. 1a).

The fitness of the phototrophic community relied on metabolic cross-feeding, also known as 'leaky capabilities'[18], characteristics that have been linked to coevolution[19]. *i*CZ-CvSc(1748) accurately predicted the distribution of external resources and metabolic exchange among organisms (Fig. 1b), revealing a clear benefit for the fungus in co-culture resulting in a doubled growth rate. This is similar to hypotheses about the parasitic nature of fungi in

[1]Department of Pediatrics, University of California, San Diego, La Jolla, CA, USA. [2]Department of Chemical and Biomolecular Engineering, The Johns Hopkins University, Baltimore, MD, USA. [3]National Bioenergy Center, National Renewable Energy Laboratory, Golden, CO, USA. [4]Department of Bioengineering, University of California, San Diego, La Jolla, CA, USA. [5]Center for Microbiome Innovation, University of California, San Diego, La Jolla, CA, USA. *e-mail: kzengler@ucsd.edu

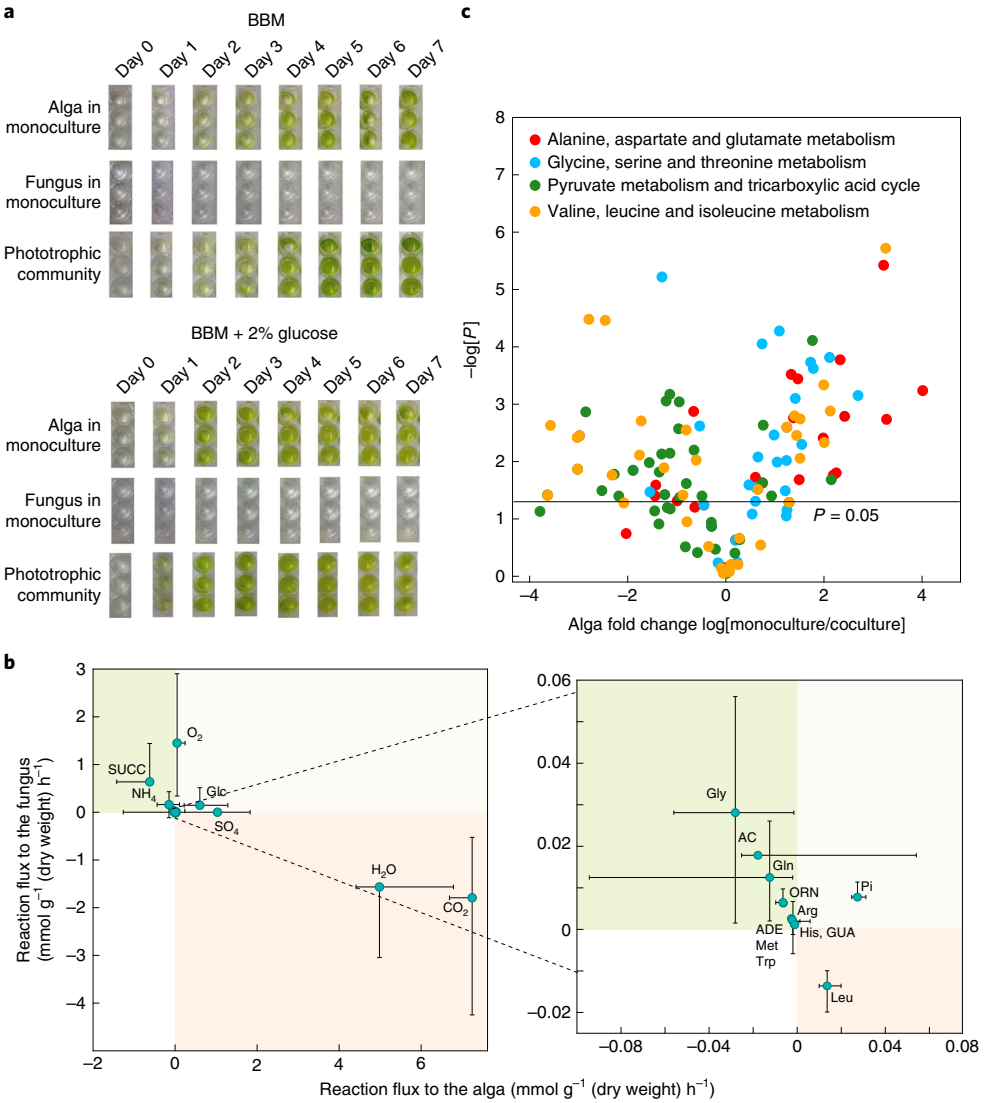

Fig. 1 | Interwoven metabolic interactions in the phototrophic community. a, The panels show the growth of individual microorganisms (that is, the alga *C. vulgaris* and the fungus *S. cerevisiae*) and the phototrophic community in Bold's basal medium (BBM) and BBM + 2% glucose. Experiments carried out with at least six replicates of biologically independent samples. **b**, Complete metabolic exchange. Error bars represent the median of predicted flux variability, while growth predictions reach at least 95% of the maximum growth rate. Flux variability was estimated using $n = 50{,}000$ warm-up points while sampling the solution space. The green area encloses metabolites produced by the alga. The pink area contains metabolites provided by the fungus. Metabolites in the pearl-white panel are supplied to the system through the culture medium. SUCC, succinate; AC, acetate; ORN, ornithine; ADE, adenosine; GUA, guanosine. **c**, Differential expression of metabolic pathways. Results obtained during the algal growth under monoculture and co-culture conditions. Upregulated and downregulated genes were determined using two-sided *t*-test, $n = 3$, and a cut-off *P* value of 0.05.

lichens[8]. Overall, the alga provides O_2 and 11 metabolites (acetate, glycine, succinate, ornithine, adenine, glutamine, methionine, guanine, histidine, arginine and tryptophan) at a total carbon flux of 0.66 mmol per g (dry weight) h^{-1} and the fungus only provides CO_2 and leucine at 0.007 mmol per g (dry weight) h^{-1} (Fig. 1b). Predicted and experimentally observed leucine uptake by the alga over all other amino acids can be associated with evolutionary tradeoffs regarding pathway topology and energetic optimization[20] as previously observed in photosynthetic microorganisms at natural environments[21]. We experimentally confirmed metabolic exchange through analysis of supernatants by target metabolomics and changes in pathways expression by RNA-sequencing data (Fig. 1c and Supplementary Fig. 2). An expanded analysis of this data is provided in Supplementary Notes. Simulations also showed that metabolic exchange is highly dynamic and community members can rapidly adapt when changing the secretion and uptake fluxes of exchanged metabolites (Supplementary Fig. 3), demonstrating all possible interactions among community members.

After we established how the phototrophic community is maintained, we evaluated the response of the growth of members to changing nutrient availability. Photobionts isolated from lichens or microbial mats can change their growth rate depending on nitrogen (for example, nitrate or amino acids)[22], CO_2 (ref. [23]), O_2 (ref. [10]) and glucose[24] availability. Our analysis suggested that there are four possible interactions among the community members: syntrophy (that is commensalism and mutualism), competition, amensalism and parasitism, and that these interactions are dependent on environmental conditions (Fig. 2 and Supplementary Fig. 1b).

CO_2, O_2, NO_3, NH_4 and glucose were determined as key drivers governing interactions. Growth phenotypes of the community

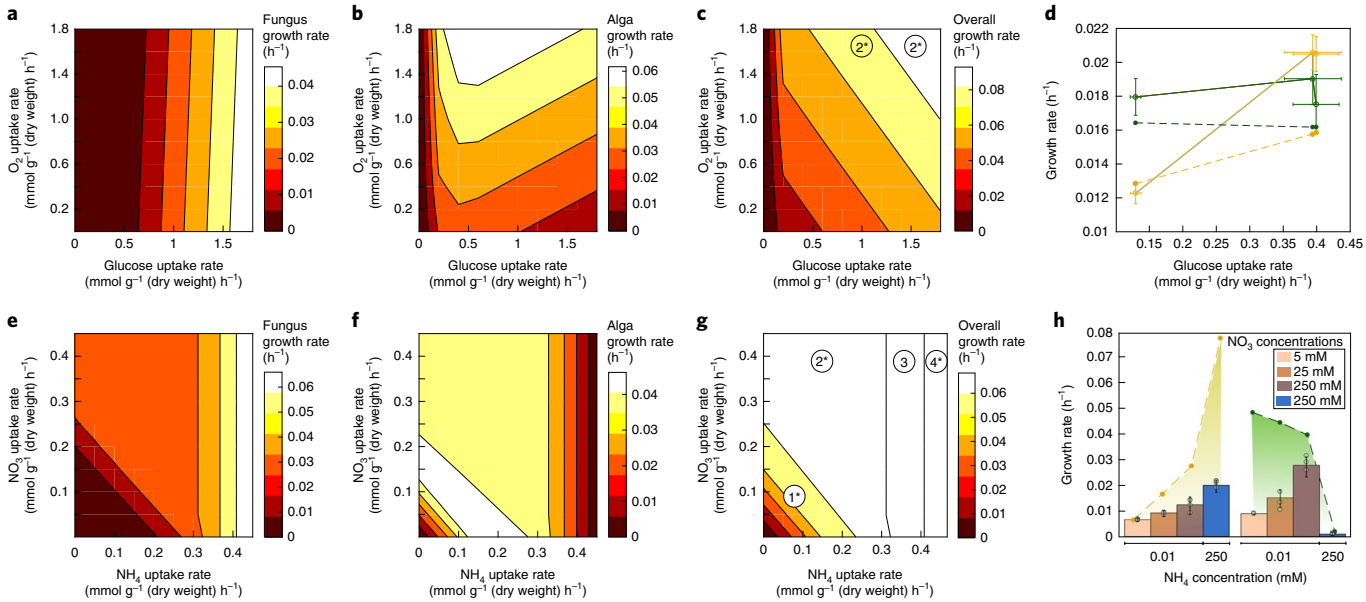

Fig. 2 | Community interactions depend on culture conditions. a,**b**, Contour plots showing predicted growth rates while varying O_2 and glucose uptake rates of the fungus (**a**) and alga (**b**) in the phototrophic community. **c**, Overall community growth rate is given by the sum of growth rates shown in **a** and **b**. Interaction types are assigned on the basis of growth-rate ratios (see Supplementary Fig. 1b). Growth-rate ratios around 1 define syntrophic interactions and ratios below 0.1 and above 10 represent amensalism. Panels labelled with a circled '2*' highlight syntrophic interactions that were experimentally validated. **d**, Growth rates at various glucose uptake rates were experimentally validated (solid lines). Predictions are shown in dotted lines and were performed by using physiologically determined glucose uptake rates of 0.14 ± 0.01 mmol g^{-1} (dry weight) h^{-1} to 0.38 ± 0.04 mmol g^{-1} (dry weight) h^{-1}. Algal experimental growth rates (green) were not significantly different (two-sided *t*-test, $P > 0.5$, $n = 3$); fungal growth rates (yellow) were statistically different (two-sided *t*-test, $P < 0.0001$, $n = 3$) as predicted. Data are mean ± s.d. **e**, Fungal predicted growth rate while varying the NH_4 and NO_3 uptake rates. **f**, Algal predicted growth rates show that high NH_4 uptake rates affected its growth. **g**, Community overall growth rate. The numbers delimit the type of interaction: 1, syntrophy (commensal); 2, syntrophy (mutualism); 3, competition; 4, amensalism or parasitism. See Supplementary Fig. 1b for further details. Asterisks indicate experimentally validated interactions. **h**, Experimental (bar plots) and predicted (dots) growth rates at different NO_3 and NH_4 concentrations for the fungus (yellow) and alga (green). Data in bar plots are mean ± s.d. of independent replicates (grey dots). Growth rates under 0.01 and 250 mM NH_4 were statistically different (two-sided *t*-test, $P < 0.0001$, $n = 3$).

members were predicted for all individual metabolites and pairwise combinations (Supplementary Fig. 4). The community formed a stable mutualistic population with a clear growth benefit for the fungus. This interaction was unwavering for all glucose and O_2 uptake rates tested in silico (Fig. 2a–c) and experimentally (Fig. 2d). Increased glucose uptake rates were beneficial for the fungus and had a slightly beneficial effect on the alga (Supplementary Fig. 4b). These predictions were confirmed experimentally (Fig. 2d and Supplementary Fig. 5) and our results showed that the growth rate of the fungus in co-culture increased at higher glucose concentration, whereas that of the alga remained constant. The fast response of the fungus to glucose can be attributed to its natural intrinsic growth rate (about 0.15 h^{-1}), which is up to one order of magnitude higher than that of the alga under optimal conditions. O_2 simulations show a proportional beneficial effect for the community members at O_2 uptake rates up to 1 mmol per g (dry weight) h^{-1} (Supplementary Fig. 4d), although when higher O_2 uptake rates were simulated the benefit was only observed for the fungus. Mono- and co-culture experiments using two different O_2 flows (0.2 and 0.4 l min^{-1}) showed that the fungus growth rate did not change significantly under monoculture (two-sided *t*-test, $P > 0.12$, $n = 4$) but under co-culture the growth rate significantly increased (13% at a flow of 0.4 l min^{-1}; two-sided *t*-test, $P < 0.05$, $n = 4$). For the alga, we experimentally observed that O_2 availability reduced the growth rate by up to 60% under monoculture and by 45% under co-culture conditions. Our predictions furthermore suggest that this negative growth effect on the alga can be abolished under certain conditions, that is, glucose uptake rate of 0.5 mmol per g (dry weight) h^{-1} and O_2 uptake rate of 1.5 mmol per g (dry weight) h^{-1} (Fig. 2b).

Different types of interactions among community members were predicted to be possible, depending on NH_4 and NO_3 uptake rates (Fig. 2e–g). NH_4 uptake rates from 0.33–0.41 mmol per g (dry weight) h^{-1} were predicted to result in the fungus dominating the community by changing its interaction with the alga from syntrophy to competition, and for NH_4 uptake rates above 0.41 mmol per g (dry weight) h^{-1} the interaction changed to amensalism or parasitism (Fig. 2g). Experimental supplementation of a low concentration of NH_4 (0.01–0.1 mM) to the culture medium, which is utilized by both partners, did not enhance the fungus growth (Fig. 2h). At this concentration, simulations show that the alga provided most of the nitrogen (flux 0.35 mmol per g (dry weight) h^{-1}) to the fungus in form of NH_4 in addition to amino acids. However, when NH_4 was added to the culture medium at a concentration of 250 mM, the fungus dominated and finally outcompeted the alga, confirming amensalism as predicted (Fig. 2h). NH_4 experiments were combined with increased NO_3 concentration from 2.5 to 250 mM, which enhanced the growth of the alga but not the fungus, since *S. cerevisiae* is unable to utilize NO_3 (Fig. 2h). Previous studies of the microalgae *Chlamydomonas reinhardtii* and *S. cerevisiae* reported similar phenotypes under high NH_4 (10 mM) conditions[13]. Experimental shift in the type of interaction was accompanied by a decrease in pH and production of ethanol. Measured ethanol concentrations at stationary phase changed from 0.43 ± 0.2 mM without NH_4 to 3.41 ± 1.0 mM once NH_4 was added. When the pH was controlled in these experiments, the alga survived longer than without pH

control, but was eventually overgrown by the fungus. Increasing supply of O_2 by bubbling air into the culture with pH control led to an improved growth of the alga as predicted (Supplementary Fig. 4d). Oxygen has a very important role across the entire community network. Out of 277 reactions containing O_2 in *i*CZ-CvSc(1748), 194 are associated with O_2 consumption and seven with O_2 production (in the alga).

Natural phototrophic communities have been shown to be sensitive to O_2 and nitrogen levels[10]. For example, high environmental levels of NH_4 during eutrophication trigger pH changes in phototrophic communities[10,25], similar to our predictions. Thus, our model can provide a quantitative tool to assess the responses of phototrophic communities to various nutrients. Additionally, this mechanistic framework enables identification and analysis of the effect of other nutrients as well as the response of phototrophic communities to eutrophication.

Phototrophic communities can change their biomass elemental composition in various environments as a function of nutrient availability (for example, nitrogen depletion)[26]. We predicted the ecological niche related to nitrogen limitations by constraining *i*CZ-CvSc(1748) with six different biomass compositions experimentally determined over the course of growth[27]. Changes in the biomass composition of the phototroph have distinct effects on the community members in mono- and co-culture. For example, the alga growth rate in monoculture was reduced by approximately 40% once nitrogen was depleted from the medium[27]. In the phototrophic community however, the growth rates of the community members remained stable varying by only about 10% compared with monoculture after nitrogen depletion (Fig. 3a). The ability to cope with nutrient depletion differently in mono- and co-culture could provide insights into the ability of phototrophic communities to thrive in harsh conditions. Our analysis demonstrates how the community equalizes and tunes its metabolism and cross-feeding in response to resource availability (Fig. 3b,c). Simulations revealed that metabolites exchanged are highly conserved and independent of the alga-to-fungus growth ratio in the community (Supplementary Fig. 6). Only the flux exchange of O_2, succinate, ornithine, glutamine, ribose and tryptophan and secreted metabolites that are part of overflow metabolism (that is production of formate, ethanol and acetate) varied in accordance with the community biomass composition. Overflow metabolism is currently poorly understood, even for axenic cultures[28,29]. It utilizes reducing equivalents and energy carriers to synthesize these side products instead of biomass[28]. Overflow metabolism in *S. cerevisiae* and heterotrophic microbial communities has been associated with excess carbon supply[30], and lichenized fungi have been found to become tolerant to overflow metabolites[31].

Natural environments provide ample probability of interplay and exchange of metabolites. We thus elucidated the growth-limiting metabolites in mono- and co-culture conditions by studying the impact of all metabolites in the model (2,965) on the entire network (Supplementary Fig. 7). Predictions were performed for six biomass compositions. Negative values indicate metabolites limiting the growth rate[32]. Predictions clustered by culture condition instead of biomass composition and showed that the alga responds differently to metabolite supplementation in 60% of the cases. The analysis also highlighted that the metabolic network of mono- and co-culture respond differently to the same metabolite (Fig. 3b). Predictions suggest that the fungus supports the alga to bypass metabolic limitations in the synthesis of certain coenzymes and precursors (plastoquinone, pantothenate and coenzyme A) (Supplementary Table 5). When the fungus grows in monoculture, cells are limited by valine, tyrosine, tryptophan and potentially butanal, but in co-culture, these metabolites may be provided by the alga. We also predicted differences in the requirements of riboflavin and 4-hydroxybenzoate between mono- and co-culture for the alga. To verify these predictions, we experimentally evaluated the effect of these metabolites on growth in mono- and co-culture (Supplementary Fig. 8). Valine, tyrosine and tryptophan improved the growth of the fungus as predicted, whereas riboflavin and butanal only benefited the alga or the fungus, respectively. Of note, tyrosine and 4-hydroxybenzoate additions had a toxic effect on the alga in both conditions, suggesting that phototrophic communities can be more resilient to toxic compounds than their individual partners. Overall, the model demonstrated accuracy of 0.69 for growth phenotype prediction on the metabolites tested (Supplementary Fig. 8c). Our results further demonstrate that data obtained for monocultures cannot readily be translated to phenotypes in co-cultures or even larger communities and exemplify current challenges in manipulating and engineering microbial communities.

Two key questions in evolutionary biology address how biological systems become genetically stable without members outcompeting themselves[33] and how communities manage deleterious gene loss to attain streamlined genomes[34]. We predicted the essentiality of 3,496 metabolic genes in mono- and co-culture. Previous results suggested that metabolic genes exhibit higher level of phenotypic variation[35], triggering adaptive benefits to an organism[36,37]. We found that both partners compensate for loss of gene functions in the other partner, contributing to the survival of the community. However, this compensation depends on the community growth stage and biomass composition (Supplementary Fig. 9). The number of essential genes required for growth in co-culture was reduced by 39% (from 194 to 115) for the alga and by 31% (from 106 to 73) for the fungus (Supplementary Fig. 10 and Supplementary Tables 6–8).

On the basis of model simulations, nine fungal mutants that changed their growth phenotypes under mono- and co-culture were selected for experimental validation. Seven mutants (systematic gene name is shown, followed by synonym in parentheses) with essential genotypes were associated with fructose and mannose metabolism (*YDL055C* (*PSA1*$^-$); *YFL045C* (*SEC53*$^-$); *YER003C* (*PMI40*$^-$)), glutamine metabolism (*YPR035W* (*GLN1*$^-$)), phospholipid biosynthesis (*YBR029C* (*CDS1*$^-$)), riboflavin metabolism (*YBR153W* (*RIB7*$^-$)) and sterol metabolism (*YHR007C* (*ERG11*$^-$)), and two mutants with non-essential genotypes were associated with oxidative phosphorylation (*YAL012W* (*CYS3*$^-$)) and methionine metabolism (*YKL055C* (*OAR1*$^-$)). Six of the seven predicted essential fungal knockouts (KOs) were rescued when grown in co-culture, confirming our predictions (Fig. 4a,b and Supplementary Table 9). The recovery of essential gene loss by the community sheds light on the lack of cultivability routinely observed from environmental samples[38].

Predictions showed that each gene deletion reshaped the distribution of nutrients across community members, triggering changes to the metabolic exchange (Fig. 4c). For example, the co-culture with *YPR035W* (*GLN1*$^-$) showed a strong benefit for the fungus at the expense of the alga by expanding the number of metabolites exchanged. Furthermore, we found that fungus KOs can also have a negative effect on the alga growth. For example, experimental results showed that the KO (*YDL055C* (*PSA1*$^-$)) reduced alga growth by 75%. Modelling predictions indicated that this growth phenotype is attained under high secretion fluxes of formate by the fungus and high acetate flux by the alga (Supplementary Fig. 10d), probably activating regulatory effects associated with stress conditions. Our simulations are consistent with metabolomics studies of microbial mats, in which abundance of metabolites such as formate, ethanol and acetate, different sugars and amino acids, change depending on environment conditions[39]. Experimental results for the two non-essential gene KOs generally agreed with our predictions. A permutation test analysis comparing experimental and predicted growth phenotypes suggested that the model could accurately predict up to 80% of the phenotypes (Supplementary Fig. 11).

Surprisingly, we also identified 50 KOs for the alga and 37 KOs for the fungus that improved the growth of the partners by

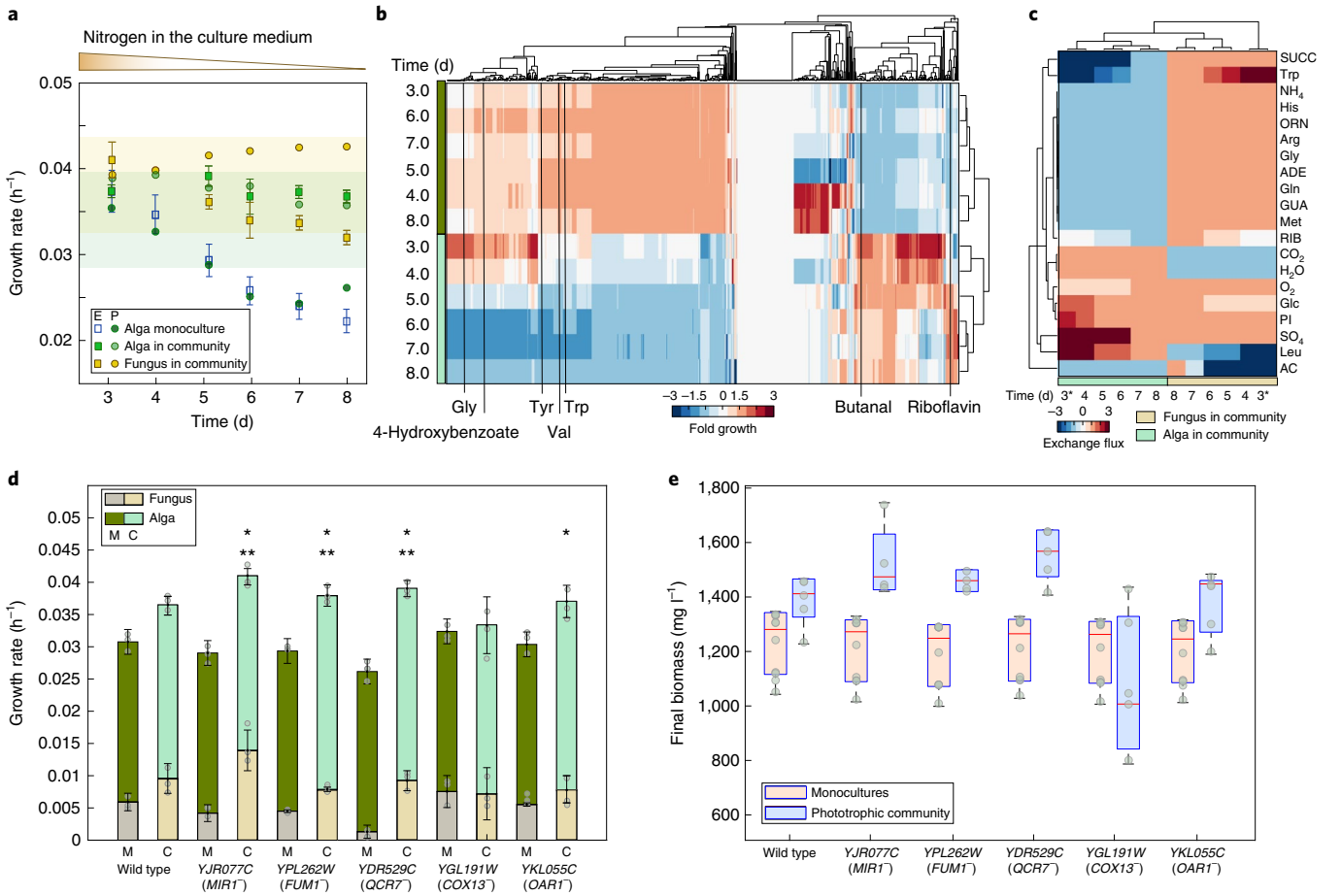

Fig. 3 | Nitrate availability and genetic drift stimulate community cooperation. a, Experimental (E) and predicted (P) growth rates of the alga in monoculture and the community under nitrogen limitation. Growth data for all conditions are provided in Supplementary Table 4. Experiments carried out by triplicate using biologically independent samples. Data are mean ± s.d. **b**, Predicted shadow prices under different biomass compositions of the alga (dark green, monoculture; light green, co-culture). Metabolites limiting, increasing and without effect on the growth rate are shown in blue, red and white, respectively. The named metabolites were tested experimentally. **c**, Predicted metabolic exchange by the community over the course of growth. RIB, ribose. **d**, Fungus knockouts with enhanced growth phenotypes were experimentally tested, showing a significant increase of the community growth rate (*MIR1*$^-$, *FUM1*$^-$, *QCR7*$^-$ and *OAR1*$^-$) of up to 15% in comparison with the co-culture of wild-type strains (two-sided *t*-test, $^{**}P < 0.05$, $n = 3$). Growth rates were determined by cell counts over the course of growth for monoculture (M) and co-culture (C) conditions. The fungus grew significantly faster under co-culture conditions than in monoculture (two-sided *t*-test, $^{*}P < 0.05$, $n = 3$). Data are mean ± s.d. of three biologically independent replicates (grey dots). **e**, The box plots show the final biomass concentration measured by dry weight at the end of the experiments for all treatments (KO). Box plots indicate the sum of experimentally determined final biomass under monoculture conditions (orange) and the final biomass of the community (blue). The central mark indicates the median of at least six independent biological replicates (grey dots), and the bottom and top edges of the box indicate the 25th and 75th percentiles, respectively. The whiskers extend to the most extreme data points not considered outliers.

shifting the available metabolic resources from one member to another (Supplementary Tables 10 and 11). Knocking out YDR529C (*QCR7*$^-$), YJR077C (*MIR1*$^-$), YKL055C (*OAR1*$^-$) or YPL262W (*FUM1*$^-$) was predicted to improve the overall growth rate of the phototrophic community by 15–25%. Experimental results confirmed a growth rate increase of 10–15%, indicating that KO of these genes provides an ecological advantage for the community (Fig. 3d,e). Thus, CM models can identify target genes that enable higher growth rates as observed experimentally in individual cultures[37] or in communities[40].

Predicted genotype–environment responses tune the phenotypes and metabolic exchange in a phototrophic community and highlight the interplay between the stoichiometric architecture of the community metabolic network. Our results reveal the importance of metabolic exchanges that share and optimally allocate cellular resources. Furthermore, the CM model facilitates the identification of suitable genotype–environment conditions for maintaining a phototrophic community as well as factors influencing the proliferation of specific members.

Model communities, like the one used here, are of great importance for unravelling dynamic interactions and providing a detailed mechanistic understanding of complex exchanges between community members[11]. Our conceptual framework could in principle be used to study interactions of microorganisms in their natural environment[3]. Recent advances in sequencing deliver almost complete genomes and accompanying expression data. Temporal and spatial measurements not only offer a comprehensive assessment of environmental parameters but also generate information about community structure. Combined with high quality genome-scale reconstructions, these data enable deciphering of dynamic interactions of community members in their natural environment. This information will lay the foundation for rational understanding, design and manipulation of microbial communities.

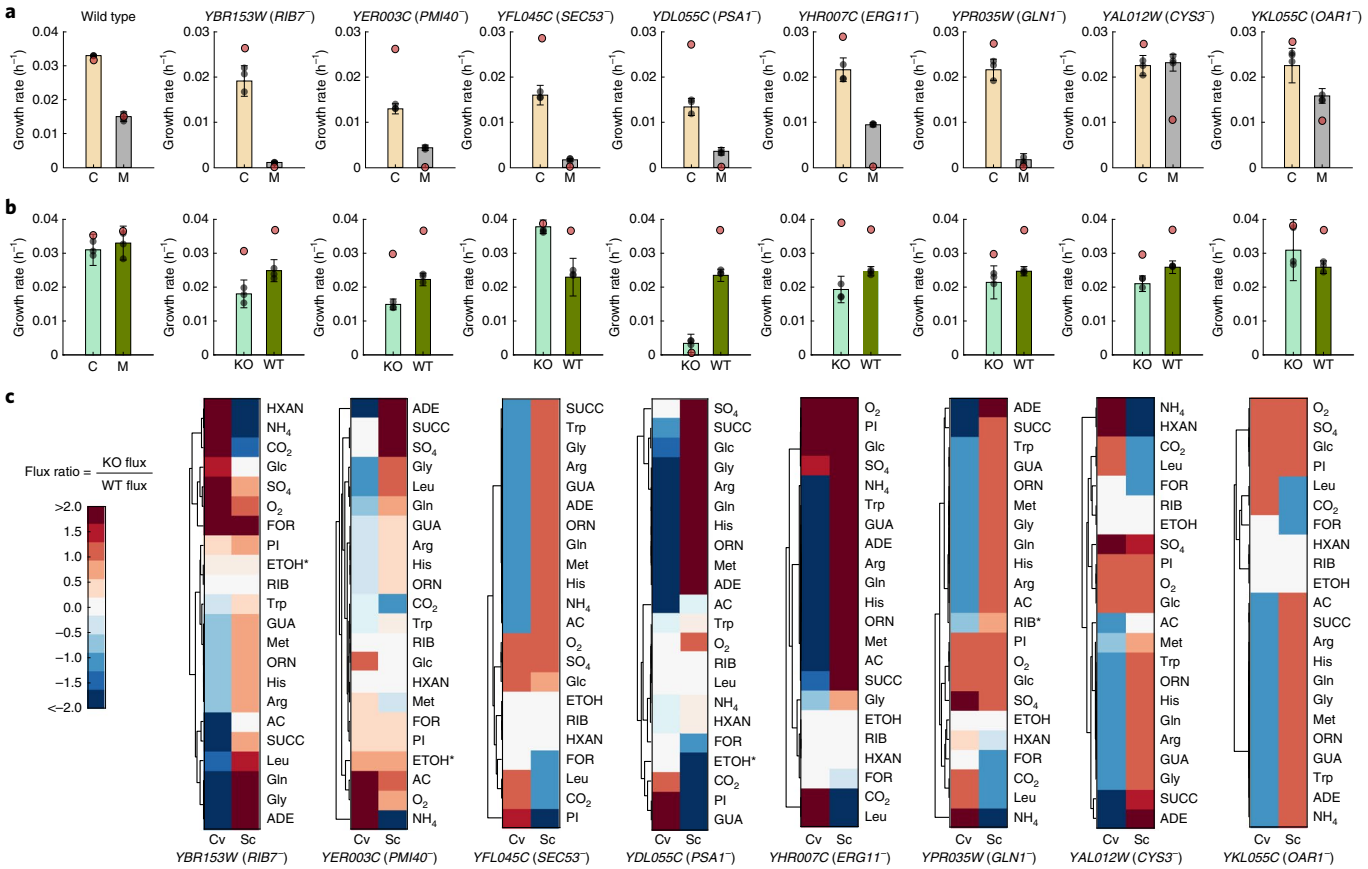

Fig. 4 | Member-specific genomic capabilities help to overcome lethal genetic gaps in the community. a, Fungal mutant strains with lethal phenotypes (*RIB7*⁻, *PMI40*⁻, *SEC53*⁻, *PSA1*⁻, *ERG11*⁻ and *GLN1*⁻) and mutants with nonlethal phenotypes (*CYS3*⁻ and *OAR1*⁻) were assayed in co-culture (C) and monoculture (M) conditions. Predicted growth phenotypes are shown with orange circles and experimental results with bar plots. Experiments were carried out using three independent biological replicates (dark dots). Data are mean ± s.d. A permutation test for heterogeneity comparison among experimental outcomes and predicted phenotypes showed an accuracy above 0.8 for modelling predictions, this result is markedly higher than would expected for a random result (~ 0.2–0.5, see Supplementary Fig. 11). Results regarding the gene *YBR029C* (CDS1⁻, phosphatidate cytidylyltransferase (CDP-diglyceride synthase) yeast specific) are shown in Supplementary Notes. **b**, Algal growth rates were determined in co-culture with each mutant strain (fungal KO) and the wild-type strain as control. **c**, Predicted metabolites exchanged for each pair condition, all fluxes were normalized by the predicted flux for the wild type. HXAN, hypoxanthine; FOR, formate; ETOH, ethanol.

Methods

Community metabolic model reconstruction. The phototrophic community model was reconstructed using the metabolic models of *C. vulgaris* UTEX 395, *i*CZ843 (ref. [16]) and *S. cerevisiae*, *i*MM904 (ref. [17]). Properties of individual and CM models are listed in Supplementary Table 1. Fields such as gene matrix and reaction localization were created de novo if missing. Naming of reactions and metabolites was adjusted to be consistent between models. After manual curation, the quality control and assessment tests for ATP, NADPH and NADH maintenance were executed for each model using the available tools in COBRA toolbox[41] and formulation in equation (1).

The models *i*CZ843 and *i*MM904 were integrated into a combined model using the COBRA toolbox as described[42]. An artificial compartment referred to as SMP[42] was created during the CM model manual curation process. The SMP defines the connectivity of individual models and the extracellular space through a common metabolite pool. Metabolites suitable for sharing were manually set (53 alga- and 164 fungus-associated metabolites) according to experimental data, such as growth curves using the BIOLOG system (Supplementary Table 2)[16,17]. Experimental data was used to set constraints on uptake of CO_2 (13.6 mmol per g (dry weight) h^{-1}), glucose (0.75 mmol per g (dry weight) h^{-1}), and other compounds (for example, nitrate, nicotinamide and pantothenate), to simulate growth of the community members (Supplementary Table 3).

Transport reactions from SMP to each microorganism were created within the boundaries shown in equation (1). Uptake or secretion fluxes through reactions associated with SMP were determined by flux balance analysis. For example, when the exchange flux of the reaction or metabolite was vital for simulating growth, the exchange reaction associated with this process carries flux, meaning that not all reactions in the SMP carry flux at the same time.

Constraints and simulation tools. Photosynthetic microbes are able to adapt and drastically change the elemental composition of their biomass (carbon, nitrogen, phosphorus, and sulfur) in response to environmental perturbations[26]. The alga *C. vulgaris* is able to adjust its elemental composition during nitrogen starvation, resulting in changes in its proteins, lipids, carbohydrates, and nucleotides[27]. *i*CZ-CvSc(1748) was constrained using six different biomass compositions, in which the available biomass compositions of the alga were alternated with the single biomass composition of the fungus[16,17]. Every pairwise biomass composition (alga–fungus) was set as an individual biomass objective function. Standard constraints, such as light, CO_2, and uptake rates of BBM components were applied to predict the overall and member-specific growth rates (Supplementary Table 3). The glucose uptake rate was calculated on the basis of experimental data obtained from the co-culture.

All CM-model simulations were performed using the Gurobi Optimizer v.5.6.3 solver (Gurobi Optimization) in the COBRA toolbox[41] for MATLAB (MathWorks). We simulated the maximal growth rate of members in the community using flux-balance analysis together with OptCom (equation (1)), an algorithm that allows the optimization of multiple objective functions at the same time considering thermodynamic, capacity and mass constraints (lb, ub and biomass stoichiometric coefficients). Although both members are considered independent and the reactions in each microorganism are mathematically assumed to have a self-governing role in every microorganism, the community growth rate results from the sum of fluxes through each member-biomass reaction. The amplitude of

metabolic fluxes (see Fig. 1b) was determined using flux variability analysis and random sampling. To uniformly sample the solution space of *i*CZ-CvSc(1748), the model was reduced as previously described and optGpSampler[16] for MATLAB with Gurobi Optimizer v.6.5.0 was used.

$$\begin{aligned} & v = v_1 + v_2 \\ & \max(c^T.v) \\ & \text{subject to S.v} = 0 \\ & lb < v < ub \end{aligned} \quad (1)$$

Transport

$$-1,000 < v < 1,000$$

Growth rates characterization and robustness analysis. The CM model was used to simulate growth rates and to predict metabolic interactions under standard conditions (Fig. 1b). The main metabolic compounds affecting community interactions were identified, that is glucose, O_2, NH_4, and NO_3 and sensitivity analysis, looking for member-specific growth responses to environmental conditions, was performed by varying uptake rates. The sensitivity analysis deploys phenotypic phase planes facilitating the observation of effects on the objective functions by varying a particular constraint[41]. Predicted growth rates in mono- and co-culture were compared with experimental results.

Environmental conditions that benefit or harm growth rates of both microorganisms in the community and monoculture were identified and corresponding media composition were determined. Flux-balance analysis solutions encompass the calculation of shadow prices, which show changes in the growth rate by simulating single supplementation for all metabolites in the metabolic network, *i*CZ-CvSc(1748). Negative shadow prices describe metabolites that are demanded or are limiting the growth rate, whereas positive values identify metabolites that are excreted in order to improve the objective value[32]. Metabolites limiting the growth were computed for all six alga models with different biomass compositions and all six co-culture models (Fig. 3b). Metabolites (that is butanal, valine, 4-hydroxybenzoate, tyrosine, tryptophan and riboflavin) predicted to affect the growth rate of individual members and the phototrophic community were tested and their effect on growth was confirmed experimentally.

A robustness analysis at different biomass compositions was performed, looking at robustness of fluxes of cross-fed metabolites and shadow prices. Simulations were carried out at controlled changes in growth rate of individual members and the community (Supplementary Fig. 7-8). A confusion matrix and various measures of quality, such as accuracy, specificity, sensitivity, positive predicted, negative predicted and Matthews correlation coefficient, were estimated according to ref. [43].

Predicting the rescue of phenotypes in gene knockouts. In silico gene deletion analysis was completed by iteratively removing reaction(s) associated with each gene in the combined model, *i*CZ-CvSc(1748), as well as for *i*CZ843 and *i*MM904. Every knockout network was used to determine the maximum growth rate of the community members. This step was iteratively performed for the six models with different biomass objective functions. Genes predicted essential and non-essential in mono- and/or co-culture were compared. Furthermore, we explored the possibility of manipulating growth rates of microorganisms in the phototrophic community by genetic modifying the fungus (knockout strains). Within this analysis we evaluated conditions as stabilizing, improving, or decreasing growth phenotypes of the community members. We also studied how the community manages to survive when the alga is co-cultured with fungus strains containing lethal traits (Fig. 4). Simulations were organized in a confusion matrix framework and the statistics and machine learning toolbox of MATLAB (MathWorks) was used to calculate 10,000 permutations (two-sided *t*-test, $P < 0.0001$) over experimentally determined and predicted growth rates of the partners in monoculture and co-culture (Supplementary Fig. 11).

Strains. *C. vulgaris* UTEX 395 (alga) was obtained from the Culture Collection of Algae at the University of Texas at Austin. Wild-type *S. cerevisiae* strain S288c (fungus) was obtained from the American Type Culture Collection (ATCC 204508). *S. cerevisiae* knockout strains (*YPR035W*, *YKL055C*, *YAL012W*, *YHR007C*, *YJR077C*, *YPL262W*, *YDR529C* and *YGL191W*) were obtained from GE Lifesciences. *S. cerevisiae* temperature-sensitive-knockout strains (*YBR153W*, *YBR029C*, *YDR341C*, *YMR208W*, *YER003C*, *YFL045C* and *YDL055C*) were provided by P. Stirling (Terry Fox Laboratory, BC Cancer Agency, Vancouver, British Columbia, Canada). Strain knockout traits, for example, standard name, essentiality phenotype and metabolic pathways, can be found in Supplementary Table 9.

Medium. Sterile BBM with 2% glucose was used to grow the community members in mono- and co-cultures. BBM consists of $NaNO_3$ (250 mg l^{-1}), KH_2PO_4 (176 mg l^{-1}), K_2HPO_4 (75 mg l^{-1}), $MgSO_4{\cdot}7H_2O$ (75 mg l^{-1}), Na_2EDTA (50 mg l^{-1}), KOH (31 mg l^{-1}), $CaCl_2{\cdot}2H_2O$ (25 mg l^{-1}), NaCl (25 mg l^{-1}), H_3BO_3 (11.4 mg l^{-1}), $FeSO_4{\cdot}7H_2O$ (4.98 mg l^{-1}), $ZnSO_4{\cdot}7H_2O$ (8.83 mg l^{-1}), H_2SO_4 (1.84 mg l^{-1}), $CuSO_4{\cdot}5H_2O$ (1.57 mg l^{-1}), $MnSO_4{\cdot}H_2O$ (1.44 mg l^{-1}), MoO_3 (0.71 mg l^{-1}) and $CoCl_2{\cdot}6H_2O$ (0.50 mg l^{-1}). The sole nitrogen source in BBM is $NaNO_3$. For some experiments, $NaNO_3$ was substituted with NH_4Cl (0.055 g l^{-1} and 13.5 g l^{-1}), that is, BBM-NH_3. Specific growth effects were tested by adding glycerol, butanal, valine, 4-hydroxybenzoate, tyrosine, tryptophan and riboflavin (1 mM each) to the medium.

Growth conditions. Standard growth tests were performed in 250 ml flasks containing 25 ml of culture medium (2% glucose in BBM medium) and the community members were inoculated at a ratio of 1:1 based on cell number. Flasks were subjected to fluorescent light (130 µmol photons m^{-2} s^{-1}) with a 12:12 h light:dark cycle. For the fungus-knockout experiments, cultures were grown in 25 ml T25 flasks containing 10 ml of autoclaved BBM with 2% glucose using a fluorescent light source with intensity of 130 µmol photons m^{-2}s^{-1} and mixed with an orbital shaker at 40 r.p.m. The pH in the medium was measured every day and 0.1 M sodium hydroxide was added to maintain a pH of 6.8. Experiments with varying nitrogen sources (NO_3 and NH_3) and added metabolites (that is butanal, valine, 4-hydroxybenzoate, tyrosine, tryptophan and riboflavin) were performed in 250 ml flasks containing 50 ml of autoclaved BBM with 2% glucose.

Analytical methods. Glucose concentrations were measured with an YSI 2700 analyser (YSI). NO_3 and NH_3 were measured with a nitrite-nitrate assay kit (Sigma) and ammonium assay kit (Megazyme), respectively. Cell counts for the community members were determined by flow cytometry. Metabolomic analysis was performed as previously reported[44]. RNA extraction, library generation and sequencing were performed by harvesting and snap-freezing cells in liquid nitrogen in biological triplicates for each condition. Cell lysates were prepared by grinding the frozen cell pellets in liquid nitrogen with 400 µl of RLT buffer (Qiagen RNeasy kit). RNA was stabilized by the addition of 2 ml Trizol reagent (Thermo Fisher Scientific) to each 1 ml of lysate. Total RNA was extracted using the RNeasy kit (Qiagen). mRNA was enriched using the Dynabeads mRNA purification kit (Invitrogen). Sequencing libraries were generated using the KAPA RNA HyperPrep kit (Roche) and by following the recommended protocol. The libraries were paired-end sequenced on an Illumina HiSeq TM 4000, using 100-base pair cycle kits. The sequencing adaptors were trimmed using the trim_galore program[45]. The reads were obtained from NCBI database[46] and aligned to the *C. vulgaris* genome (Assembly No. ASM102112v1) and to the *S. cerevisiae* genome (accession No. NC_001133). Subread package-featureCounts (v.1.5.0-p1)[47] was used to determine reads for each coding region. The aligned sequencing reads (Supplementary Table 12) were used to determine RNA expression as fragments per kilobase per million. The aligned reads were also used to determine differential gene expression using DESeq2 (ref. [48]).

Reporting Summary. Further information on research design is available in the Nature Research Reporting Summary linked to this article.

Data availability

The phototrophic community model, as well as individual models are available in Supplementary Dataset 1 and are described in Supplementary Table 1. Models constrained with different biomass compositions are also provided in Supplementary Dataset 1 and described in Supplementary Table 4. Supplementary Information is also available at https://github.com/cristalzucsd/PhototrophicCommunities. All sequencing reads were deposited in the Sequence Read Archive under BioProject PRJNA496045, with specific numbers listed in Supplementary Table 12.

Code availability

Computer code will be provided upon request from the corresponding author.

Received: 1 November 2018; Accepted: 21 August 2019;
Published online: 07 October 2019

References

1. Flemming, H.-C. & Wuertz, S. Bacteria and archaea on Earth and their abundance in biofilms. *Nat. Rev. Microbiol.* **17**, 247–260 (2019).
2. Zuñiga, C., Zaramela, L. & Zengler, K. Elucidation of complexity and prediction of interactions in microbial communities. *Microb. Biotechnol.* **10**, 1500–1522 (2017).
3. Zengler, K. & Zaramela, L. S. The social network of microorganisms—how auxotrophies shape complex communities. *Nat. Rev. Microbiol.* **16**, 383–390 (2018).
4. de Vera, J.-P. et al. Survival potential and photosynthetic activity of lichens under Mars-like conditions: a laboratory study. *Astrobiology* **10**, 215–227 (2010).
5. Prieto-Barajas, C. M., Valencia-Cantero, E. & Santoyo, G. Microbial mat ecosystems: structure types, functional diversity, and biotechnological application. *Electron. J. Biotechnol.* **31**, 48–56 (2018).

6. Amin, S. A., Parker, M. S. & Armbrust, E. V. Interactions between diatoms and bacteria. *Microbiol. Mol. Biol. Rev.* **76**, 667–684 (2012).
7. Insarova, I. D. & Blagoveshchenskaya, E. Y. Lichen symbiosis: Search and recognition of partners. *Biol. Bull.* **43**, 408–418 (2016).
8. Hill, D. J. The growth of lichens with special reference to the modelling of circular thalli. *Lichenologist* **13**, 265–287 (1981).
9. Grube, M., Cardinale, M., de Castro, J. V., Müller, H. & Berg, G. Species-specific structural and functional diversity of bacterial communities in lichen symbioses. *ISME J.* **3**, 1105–1115 (2009).
10. Bolhuis, H., Cretoiu, M. S. & Stal, L. J. Molecular ecology of microbial mats. *FEMS Microbiol. Ecol.* **90**, 335–350 (2014).
11. Zhalnina, K., Zengler, K., Newman, D. & Northen, T. R. Need for laboratory ecosystems to unravel the structures and functions of soil microbial communities mediated by chemistry. *mBio* **9**, e01175-18 (2018).
12. Zengler, K. et al. EcoFABs: advancing microbiome science through standardized fabricated ecosystems. *Nat. Methods* **16**, 567–571 (2019).
13. Hom, E. F. Y. & Murray, A. W. Niche engineering demonstrates a latent capacity for fungal–algal mutualism. *Science* **345**, 94–98 (2014).
14. Li, T. et al. Mimicking lichens: incorporation of yeast strains together with sucrose-secreting cyanobacteria improves survival, growth, ROS removal, and lipid production in a stable mutualistic co-culture production platform. *Biotechnol. Biofuels* **10**, 55 (2017).
15. Zengler, K. & Palsson, B. O. A road map for the development of community systems (CoSy) biology. *Nat. Rev. Microbiol.* **10**, 366–372 (2012).
16. Zuñiga, C. et al. Genome-scale metabolic model for the green alga *Chlorella vulgaris* UTEX 395 accurately predicts phenotypes under autotrophic, heterotrophic, and mixotrophic growth conditions. *Plant Physiol.* **172**, 589–602 (2016).
17. Mo, M. L., Palsson, B. Ø. & Herrgard, M. J. Connecting extracellular metabolomic measurements to intracellular flux states in yeast. *BMC Syst. Biol.* **3**, 37 (2009).
18. Oliveira, N. M., Niehus, R. & Foster, K. R. Evolutionary limits to cooperation in microbial communities. *Proc. Natl Acad. Sci. USA* **111**, 17941–17946 (2014).
19. Guimarães, P. R., Pires, M. M., Jordano, P., Bascompte, J. & Thompson, J. N. Indirect effects drive coevolution in mutualistic networks. *Nature* **550**, 511–514 (2017).
20. Du, B., Zielinski, D. C., Monk, J. M. & Palsson, B. O. Thermodynamic favorability and pathway yield as evolutionary tradeoffs in biosynthetic pathway choice. *Proc. Natl Acad. Sci. USA* **115**, 11339–11344 (2018).
21. Stegman, M. R., Cottrell, M. T. & Kirchman, D. L. Leucine incorporation by aerobic anoxygenic phototrophic bacteria in the Delaware estuary. *ISME J.* **8**, 2339–2348 (2014).
22. Dahlman, L., Persson, J., Näsholm, T. & Palmqvist, K. Carbon and nitrogen distribution in the green algal lichens *Hypogymnia physodes* and *Platismatia glauca* in relation to nutrient supply. *Planta* **217**, 41–48 (2003).
23. Palmqvist, K., Franklin, O. & Näsholm, T. Symbiosis constraints: Strong mycobiont control limits nutrient response in lichens. *Ecol. Evol.* **7**, 7420–7433 (2017).
24. Goff, L. J. (ed.). *Algal symbiosis: a continuum of interaction strategies* (Cambridge Univ. Press, 2011).
25. Jovan, S., Riddell, J., Padgett, P. E. & Nash, T. H. Eutrophic lichens respond to multiple forms of N: implications for critical levels and critical loads research. *Ecol. Appl.* **22**, 1910–1922 (2012).
26. Navarrete, A. et al. Physiological status and community composition of microbial mats of the Ebro Delta, Spain, by signature lipid biomarkers. *Microb. Ecol.* **39**, 92–99 (2000).
27. Zuñiga, C. et al. Predicting dynamic metabolic demands in the photosynthetic eukaryote *Chlorella vulgaris*. *Plant Physiol.* **176**, 450–462 (2018).
28. Basan, M. et al. Overflow metabolism in *Escherichia coli* results from efficient proteome allocation. *Nature* **528**, 99–104 (2015).
29. Liu, J. K. et al. Predicting proteome allocation, overflow metabolism, and metal requirements in a model acetogen. *PLOS Comput. Biol.* **15**, e1006848 (2019).
30. Klitgord, N. & Segrè, D. Environments that induce synthetic microbial ecosystems. *PLoS Comput. Biol.* **6**, e1001002 (2010).
31. Wink, M. Evolution of secondary metabolites from an ecological and molecular phylogenetic perspective. *Phytochemistry* **64**, 3–19 (2003).
32. Reznik, E., Mehta, P. & Segrè, D. Flux imbalance analysis and the sensitivity of cellular growth to changes in metabolite pools. *PLoS Comput. Biol.* **9**, e1003195 (2013).
33. Rakoff-Nahoum, S., Foster, K. R. & Comstock, L. E. The evolution of cooperation within the gut microbiota. *Nature* **533**, 255–259 (2016).
34. Morris, J. J., Lenski, R. E. & Zinser, E. R. The black queen hypothesis: evolution of dependencies through adaptive gene loss. *mBio* **3**, e00036-12 (2012).
35. Ackermann, M. A functional perspective on phenotypic heterogeneity in microorganisms. *Nat. Rev. Microbiol.* **13**, 497–508 (2015).
36. Good, B. H., McDonald, M. J., Barrick, J. E., Lenski, R. E. & Desai, M. M. The dynamics of molecular evolution over 60,000 generations. *Nature* **551**, 45–50 (2017).
37. Breslow, D. K. et al. A comprehensive strategy enabling high-resolution functional analysis of the yeast genome. *Nat. Methods* **5**, 711–718 (2008).
38. Zengler, K. et al. Cultivating the uncultured. *Proc. Natl Acad. Sci. USA* **99**, 15681–15686 (2002).
39. Kim, Y.-M. et al. Diel metabolomics analysis of a hot spring chlorophototrophic microbial mat leads to new hypotheses of community member metabolisms. *Front. Microbiol.* **6**, 209 (2015).
40. Lynch, M. Streamlining and simplification of microbial genome architecture. *Annu. Rev. Microbiol.* **60**, 327–349 (2006).
41. Schellenberger, J. et al. Quantitative prediction of cellular metabolism with constraint-based models: the COBRA Toolbox v2.0. *Nat. Protoc.* **6**, 1290–1307 (2011).
42. Nagarajan, H. et al. Characterization and modelling of interspecies electron transfer mechanisms and microbial community dynamics of a syntrophic association. *Nat. Commun.* **4**, 2809 (2013).
43. Matthews, B. W. Comparison of the predicted and observed secondary structure of T4 phage lysozyme. *Biochim. Biophys. Acta* **405**, 442–451 (1975).
44. Henard, C. A., Guarnieri, M. T. & Knoshaug, E. P. The *Chlorella vulgaris* *S*-nitrosoproteome under nitrogen-replete and -deplete conditions. *Front. Bioeng. Biotechnol.* **4**, 100 (2017).
45. Krueger, F. *Trim Galore!: A Wrapper Tool Around Cutadapt and FastQC to Consistently Apply Quality and Adapter Trimming to FastQ Files* https://www.bioinformatics.babraham.ac.uk/projects/trim_galore/ (2015).
46. Agarwala, R. et al. Database resources of the National Center for Biotechnology Information. *Nucleic Acids Res.* **46**, D8–D13 (2018).
47. Liao, Y., Smyth, G. K. & Shi, W. featureCounts: an efficient general purpose program for assigning sequence reads to genomic features. *Bioinformatics* **30**, 923–930 (2014).
48. Love, M. I., Huber, W. & Anders, S. Moderated estimation of fold change and dispersion for RNA-seq data with DESeq2. *Genome Biol.* **15**, 550 (2014).

Acknowledgements

We acknowledge P. Stirling at the T. Fox Laboratory and P. Hieter and M. Smith Laboratories at the University of British Columbia, Vancouver, Canada for kindly providing several fungal strains. We also acknowledge D. Zielinski at University of California, San Diego for providing input at all stages of this work. This material is based on work supported by the National Science Foundation under Awards 1332344 and CBET-1804187 and the U.S. Department of Energy (DOE), Office of Science, Office of Biological and Environmental Research under Awards DE-SC0012658 and DE-SC0019388. C.Z. was in part supported by Mexican National Research Council, CONACYT, fellowship No. 237897.

Author contributions

C.Z., M.J.B. and K.Z. conceived the study. C.Z. developed computational methods, performed simulations and designed experiments. C.-T.L. and G.Y. performed physiological experiments regarding community stability. M.G. generated metabolomics data. M.M.A.-B. generated RNA-sequencing data. T.-T.L., L.J. and L.Z. performed additional experiments and computational analyses. C.Z. compiled and analysed modelling and experimental outcomes. C.Z. and K.Z. wrote the manuscript with input from all co-authors.

Competing interests

The authors declare no competing interests.

Additional information

Supplementary information is available for this paper at https://doi.org/10.1038/s41564-019-0567-6.

Correspondence and requests for materials should be addressed to K.Z.

nature research

Corresponding author(s): Karsten Zengler

Last updated by author(s): Jul 25,2019

Reporting Summary

Nature Research wishes to improve the reproducibility of the work that we publish. This form provides structure for consistency and transparency in reporting. For further information on Nature Research policies, see Authors & Referees and the Editorial Policy Checklist.

Statistics

For all statistical analyses, confirm that the following items are present in the figure legend, table legend, main text, or Methods section.

n/a	Confirmed	
☐	☒	The exact sample size (*n*) for each experimental group/condition, given as a discrete number and unit of measurement
☐	☒	A statement on whether measurements were taken from distinct samples or whether the same sample was measured repeatedly
☐	☒	The statistical test(s) used AND whether they are one- or two-sided *Only common tests should be described solely by name; describe more complex techniques in the Methods section.*
☒	☐	A description of all covariates tested
☐	☒	A description of any assumptions or corrections, such as tests of normality and adjustment for multiple comparisons
☐	☒	A full description of the statistical parameters including central tendency (e.g. means) or other basic estimates (e.g. regression coefficient) AND variation (e.g. standard deviation) or associated estimates of uncertainty (e.g. confidence intervals)
☐	☒	For null hypothesis testing, the test statistic (e.g. *F*, *t*, *r*) with confidence intervals, effect sizes, degrees of freedom and *P* value noted *Give P values as exact values whenever suitable.*
☒	☐	For Bayesian analysis, information on the choice of priors and Markov chain Monte Carlo settings
☒	☐	For hierarchical and complex designs, identification of the appropriate level for tests and full reporting of outcomes
☒	☐	Estimates of effect sizes (e.g. Cohen's *d*, Pearson's *r*), indicating how they were calculated

Our web collection on statistics for biologists contains articles on many of the points above.

Software and code

Policy information about availability of computer code

Data collection	Physiological data was collected from experiments carried out in biologically independent triplicates. The reads were aligned to the C. vulgaris genome (Assembly No. ASM102112v1) and to the S. cerevisiae genome (accession No. NC_001133). Subread package-featureCounts (version 1.5.0-p1) 11 was used to determine reads per each coding region. The aligned sequencing reads were used to determine RNA expression as fragments per kilobase per million. The aligned reads were also used to determine differential gene expression using DESeq2.
Data analysis	Model simulations were performed using the Gurobi Optimizer Version 5.6.3 solver (Gurobi Optimization Inc., Houston, Texas) in the COBRA Toolbox 3 for MATLAB R2017b (The MathWorks Inc., Natick, MA)

For manuscripts utilizing custom algorithms or software that are central to the research but not yet described in published literature, software must be made available to editors/reviewers. We strongly encourage code deposition in a community repository (e.g. GitHub). See the Nature Research guidelines for submitting code & software for further information.

Data

Policy information about availability of data

All manuscripts must include a data availability statement. This statement should provide the following information, where applicable:

- Accession codes, unique identifiers, or web links for publicly available datasets
- A list of figures that have associated raw data
- A description of any restrictions on data availability

The phototrophic community model (CM-model) as well as individual models (M-models) are available in Supplementary Dataset 1 and described in Supplementary Table 1. Models constrained with different biomass compositions are also provided in Supplementary Dataset 1 and described in Supplementary Table 4. Dataset 1 is available in the Github repository https://github.com/cristalzucsd/PhototrophicCommunities. Additionally, all sequencing reads is available in the Sequence Read Archive under BioProject PRJNA496045, with specific numbers listed in Supplementary Table 12.

Field-specific reporting

Please select the one below that is the best fit for your research. If you are not sure, read the appropriate sections before making your selection.

☐ Life sciences ☐ Behavioural & social sciences ☒ Ecological, evolutionary & environmental sciences

For a reference copy of the document with all sections, see nature.com/documents/nr-reporting-summary-flat.pdf

Ecological, evolutionary & environmental sciences study design

All studies must disclose on these points even when the disclosure is negative.

Study description	Determination of cellular communication in a phototrophic community, integrating metatranscriptomics, metabolomics, and phenotyping with computational modeling.
Research sample	Samples of the phototrophic community composed of the photobiont, C. vulgaris, and the mycobiont, S. cerevisiae, and individual members were subjected to different treatments e.g. nutrients addition (43 conditions), target metabolomics and metatranscriptomics (2 conditions), and knock-outs (13).
Sampling strategy	Not applicable. The experimental design for all treatments did not test for interactions between treatments.
Data collection	Geng Yu, Chien-Ting Li, Ting-Ting Li, and Liqun Jiang collected the data in a systematic matter to evaluate the response variables such as growth and metabolites concentration. In the case of RNA-seq data the samples were collected by Chien-Ting Li during the bionts exponential phase under monoculture and coculture conditions.
Timing and spatial scale	Not applicable. Samples were taken in steady state.
Data exclusions	Data was not excluded
Reproducibility	All experiments, metatranscriptomics, metabolomics, and phenotypic of gene knock-outs, were carried out at least in triplicate.
Randomization	Not applicable.
Blinding	No blinding was done in this study. Experiments were model-driven and data are quantitative, most measurements are made using a machine, and not easily subject to operator bias.

Did the study involve field work? ☐ Yes ☒ No

Reporting for specific materials, systems and methods

We require information from authors about some types of materials, experimental systems and methods used in many studies. Here, indicate whether each material, system or method listed is relevant to your study. If you are not sure if a list item applies to your research, read the appropriate section before selecting a response.

Materials & experimental systems

n/a	Involved in the study
☒	☐ Antibodies
☒	☐ Eukaryotic cell lines
☒	☐ Palaeontology
☒	☐ Animals and other organisms
☒	☐ Human research participants
☒	☐ Clinical data

Methods

n/a	Involved in the study
☒	☐ ChIP-seq
☒	☐ Flow cytometry
☒	☐ MRI-based neuroimaging